Atmos. Chem. Phys. Discuss., 11, 531–566, 2011
www.atmos-chem-phys-discuss.net/11/531/2011/
doi:10.5194/acpd-11-531-2011

Atmospheric Chemistry and Physics Discussions

The fluorescence properties of aerosol larger than 0.8 µm in an urban and a PBA-dominated location

A. M. Gabey[1], W. R. Stanley[2], M. W. Gallagher[1], and P. H. Kaye[2]

[1]Centre for Atmospheric Science, University of Manchester, UK
[2]Science and Technology Research Institute, University of Hertfordshire, UK

Received: 21 October 2010 – Accepted: 21 December 2010 – Published: 7 January 2011

Correspondence to: A. M. Gabey (andrew.m.gabey@postgrad.manchester.ac.uk)

Published by Copernicus Publications on behalf of the European Geosciences Union.

Abstract

Dual-wavelength Ultraviolet light-induced fluorescence (UV-LIF) measurements were performed on ambient environmental aerosol in Manchester, UK (urban city centre, winter) and Borneo, Malaysia (remote, tropical), which are taken to represent environments with negligible and significant primary biological aerosol (PBA) influences, respectively. Single-particle fluorescence intensity and optical equivalent diameter were measured with a Wide Issue Bioaerosol Sensor, version 3 (WIBS3) in the diameter range 0.8 µm≤D_P≤20 µm for 2–3 weeks and filters were analysed using energy dispersive X-ray (EDX) spectroscopy, which revealed mostly non-PBA dominated particle sizes larger than 1 µm in Manchester.

The WIBS3 features three fluorescence channels: Fluorescence excited at 280 nm is recorded at 310–400 nm and 400–600 nm and fluorescence excited at 370 nm is detected at 400–600 nm. In Manchester the primary size mode of fluorescent and non-fluorescent material was at 1.2 µm. In Borneo non-fluorescent material peaked at 1.2 µm and fluorescent at 3–4 µm. The fluorescence intensity at 400–600 nm generally increased with D_P at both sites, as did the 310–400 nm intensity in Borneo. In Manchester the 310–400 m fluorescence decreased at D_P>4 µm, suggesting this channel offers additional discrimination between fluorescent particle types. Finally, the ratio of fluorescence intensity in two pairs of channels was investigated as a function of particle diameter and this varied significantly between the two environments, demonstrating that the fluorescent aerosol in each can in principle be distinguished using a combination of fluorescence and elastic scattering measurements.

1 Introduction

Primary Biological Aerosol (PBA) is the subset of the atmospheric aerosol that is comprised of anything discernibly biological in nature, including plant and insect debris, fungal and plant spores, pollens, cells, viruses and bacteria. Its abundance in the

ACPD
11, 531–566, 2011

atmosphere is poorly constrained and potential feedback on cloud-hydrological pathways is not yet included in climate models. Its transport has implications for global biodiversity and disease transmission and there are potential effects on cloud microphysical processes because of the ability of PBA to act as "giant" cloud condensation nuclei (CCN) and heterogeneous ice nuclei (IN) at temperatures up to −2 °C (Diehl et al., 2001, 2002). In rural areas the PBA is dominated by fungal spores whereas urban locations usually contain a more varied PBA population thought to contain a larger bacterial component (Matthias-Maser and Jaenicke, 1995) because of influences such as municipal waste treatment plants.

1.1 PBA fluorescence

Many PBA contain compounds such as certain aromatic amino acids that are so-called "bio-fluorophores". These molecules emit fluorescence when excited at the appropriate wavelength. The absorption cross-section and fluorescence quantum yield of these compounds are large enough that, despite the fact they typically account for ∼5% of the PBA dry mass (e.g., Faris et al., 1997) their emission dominates the fluorescence from the entire particle. The most consistently fluorescent bio-fluorophores include the co-enzyme NAD(P)H, part of the metabolic process, and the amino acid Tryptophan. The excitation peak of Tryptophan lies near 280 nm and its fluorescence is emitted primarily at 300–400 nm. NADH is excited between 270 and 400 nm and fluorescence occurs between 400 and 600 nm. Riboflavin is excited at 300–500 nm and emits mostly between 400 and 700 nm (e.g., Lakowicz, 2006; Kaye et al., 2005; Hill et al., 2009). The excitation and emission bands of these bio-fluorophores are quite well separated therefore this fluorescence can be used to separate PBA from ambient aerosol. This technique brings near real-time measurements compared with biochemical analyses and the ability to monitor concentrations for long periods with no additional resources required.

Laboratory measurements (Agranovski et al., 2003a) and field tests (Ho, 1996) using the TSI Ultraviolet Aerodynamic Particle Sizer (UV-APS/FLAPS) to investigate

ACPD
11, 531–566, 2011

various bacteria and spores demonstrate that a large proportion of PBA are detected successfully by UV-LIF at wavelengths corresponding to NAD(P)H. It has also been demonstrated that discrimination between certain fluorescent particle types (e.g. fungal spores and bacteria) can be achieved by comparing the fluorescence spectra of particles after excitations at multiple wavelengths (e.g., Sivaprakasam et al., 2007) although the spectra of different biological species do not vary significantly. More recently, Pan et al. (2010) used computational processes with data from fluorescence-based detection systems to discriminate PBA from environmental aerosol by comparing the fluorescence spectra of ambient aerosol particles with those measured in the laboratory.

1.2 Factors affecting PBA fluorescence

A number of factors affect the intensity of fluorescence from a PBA particle: The intensity of NAD(P)H-related fluorescence from bacteria varies depending on its physiological age, the stage in its lifecycle and the environmental stresses such as heat or low humidity that the sample is subjected to (Agranovski et al., 2003b). Bio-chemical interactions within cells also affect the fluorescence quantum yield from fluorophores. One example of this is NADH, which emits higher-intensity fluorescence when bound to proteins (Lakowicz, 2006). Uk Lee et al. (2010) note that ending the biological activity in fungal spores using a thermal shock of 400 °C does not immediately affect their fluorescence intensity when measured with a UV-APS. This demonstrates that it is the breakdown or depletion of bio-fluorophores over longer timescales that affect fluorescence intensity.

The presence of liquid water inside or coating a PBA also affects the measured fluorescence from it. This is noteworthy because pollen (e.g., Diehl et al., 2001), bacterial spores (e.g., Westphal et al., 2003) and fungal spores (e.g., Yarwood, 1950) are known to take up water vapour from sub-saturated air. Faris et al. (1997) carried out single-particle measurements on aqueous and dry Bacillus Subtilis spores and showed that the fluorescence cross-section of wet particles was 25% lower than for dry particles

ACPD
11, 531–566, 2011

when UV energy fluence was less than 1.3 mJ cm^{-2}.

1.3 Interferents

Fluorescent non-PBA also exists in the atmosphere, some of which possesses similar fluorescence properties to those of PBA. One example is combustion aerosol, which contains fluorescent Polycyclic Aromatic Hydrocarbons (PAHs). This increases the likelihood of UV-LIF reporting false positives in some environments. While combustion contributes mostly small aerosol particles, these readily agglomerate into larger particles. Schauer et al. (2004) note that the PAHs found in $PM_{2.5}$ material are dominated by fresh local combustion emissions. Humic and Fulvic acids (found in soil dust) also share these fluorescence properties and are formed during the decomposition of biomass. The suspension of soil dust favours the coarse mode over smaller particles, providing another source of coarse mode fluorescent material.

1.4 Past urban and tropical rainforest PBA measurements

The difficulty associated with performing measurements with standard biological samplers means few estimates of total PBA in a given environment exist. Matthias-Maser and Jaenicke (1995) performed optical and electron microscope analyses of filter measurements recorded in Mainz, Germany, a site influenced alternately by urban and rural fetches. During urban influence in May 1995 bacteria, sized 0.6–2 µm, dominated the PBA and numbered $\sim 3\times10^3$ l^{-1}, representing 20–30% of the total aerosol number. PBA number fraction varied between 1–20% at larger sizes. In contrast the rural-influenced PBA was dominated by pollen and spores. Gilbert and Reynolds (2005) captured and counted fungal spores on glass slides coated with petroleum jelly in the understorey of a tropical forest in Queensland, Australia, and found a strong diurnal cycle with concentrations ranging from $\sim10^2$ l^{-1} in daylight to $\sim10^3$ l^{-1} at night with a similar, albeit weaker, cycle observed within the canopy.

ACPD
11, 531–566, 2011

1.5 Past fluorescent PBA measurements

A small number of studies have been carried out on ambient fluorescent aerosol: Huffman et al. (2010) measured the ambient aerosol in Mainz, Germany, for several months in the autumn of 2006 using a TSI UVAPS. They report modes in the fluorescent size distribution at aerodynamic diameter intervals 0.7–0.9 µm and 3–5 µm, with fluorescent particles accounting for 20–30% of particles at D_a>3 µm. They also conclude that PAHs are likely to dominate only the sub-1 µm mode. The continuous fluorescence spectra of individual ambient coarse-mode particles (Pinnick et al., 1999, 2004; Pan et al., 2007) exhibit a surprising lack of variation, with ten template spectra able to describe more than 90% of the spectra obtained in urban, semi-urban and desert environments. Gabey et al. (2010) used a WIBS3 (described later in the text) to monitor particle fluorescence using two excitation and detection wavelengths corresponding to Tryptophan and NADH to measure the particle number above and below a tropical rainforest canopy in Borneo, Malaysia. They found a strong diurnal cycle below the canopy but not above, with $\sim 10^3$ fluorescent particles l^{-1} below the canopy and $\sim 2\times 10^2$ l^{-1} above, suggesting the source was fungal spores generated mainly within the canopy trunk space and in the forest litter zone.

1.6 Scope

This work attempts to identify the likely nature of fluorescent aerosol in Manchester, UK in December 2009 and compares the characteristics with those recorded within a tropical rainforest in Borneo, Malaysia, in June–July 2008. The morphology and composition of particles collected on Nuclepore® filters was established using an Environmental Scanning Electron Microscope (ESEM) with energy-dispersive X-ray (EDX) detector. A WIBS3 fluorescence aerosol spectrometer was used to measure the size distributions, number concentrations and fluorescence properties of ambient particles found in each environment. Using this information, we compare and contrast the fluorescent aerosol populations at each site. Finally, we use the fluorescence properties of

ACPD
11, 531–566, 2011

the PBA in Borneo to determine the number of similar particles present in Manchester.

2 Methods and instrumentation

2.1 WIBS3

The WIBS3 (Kaye et al., 2005; Foot et al., 2008) performed single-particle UV-LIF measurements at each location. Air is pumped through the instrument at 2.38 l min^{-1} with 10% drawn via a needle into a narrow stream so that aerosol moves in single-file through the centre of a sensing region. The other 90% of the air is filtered and re-introduced as a sheath flow. As a particle passes through the sensing region it encounters a 632 nm continuous-wave laser beam and the intensity of light elastically scattered forward and sideways is measured to allow particle diameter to be estimated. Two optically filtered Xenon flash-lamps then sequentially provide ultraviolet radiation centred at wavelengths of 280 nm and 370 nm with an energy fluence of 320–350 µJ cm^{-2} to each particle. A pair of spherical mirrors, each subtending 1.33 steradian, focus any fluorescence emitted by the particle onto one of two photomultiplier tubes (PMTs), each optically filtered to limit their wavelength response to 310–400 nm and 400–600 nm, respectively. The recorded fluorescence intensity for each particle is not an absolute value but directly proportional to it, therefore fluorescence intensities are stated in arbitrary units (a.u.). The intensity scale is different between channels but does not change between campaigns.

Both PMTs can record fluorescence during the 280 nm excitation because the excitation wavelength does not overlap with the detection bands. However, only the 400–600 nm PMT is able to operate during the 370 nm excitation. The excitation and detection wavelengths were chosen to correspond to the excitation and fluorescence wavebands of intrinsic bio-fluorophores Tryptophan and NAD(P)H. The optical equivalent diameter of each particle is estimated from scattered laser light by comparing the measured values with those calculated from a Mie Scattering model calibrated using

ACPD
11, 531–566, 2011

polystyrene latex microspheres (Duke Scientific, Inc.).

2.2 Electron microscopy and elemental analysis of filter samples

To supplement the Manchester WIBS3 data, a "DPS" portable PM_{10} sampler (SKC, Inc.) was placed next to the WIBS3 inlet. This sampler collected aerosol onto NuclePore® substrates (pore size 400 nm) at a flow rate of 7 l min^{-1} for a total of 26 h over three days towards the end of the campaign. ESEM (Philips XL30 ESEM-FG) was used to image the particles on the substrates. Unlike conventional SEM, ESEM uses a weaker vacuum with gaseous H_2O inside the imaging chamber so that the samples do not need to be coated before imaging. Secondary electron images were collected using the gaseous secondary electron (GSE) detector. Low-vacuum ("environmental") mode was used with a H_2O pressure of 0.5 Torr.

Elemental analysis of each particle was performed using the EDX spectrometer attached to the ESEM. In the analysis a 15 keV electron beam liberates an electron from the "K" shell of each atom in a sample. An electron transition from a higher energy level replaces the liberated electron and an X-ray photon is emitted with an energy characterised by the atomic species. This yields an energy spectrum with peaks corresponding to the dominant elements in the sample.

2.3 Data processing and particle selection criteria

Even if sampled particles display no fluorescence the WIBS3 records a finite fluorescence intensity in each channel because of internal component fluorescence. This baseline was monitored during each experiment and did not exhibit any trend or significant variation during the measurement periods. To separate genuinely fluorescent particles from these artefacts, a minimum fluorescence intensity threshold was applied. This threshold (T_i) was calculated using Eq. (1):

$$T_i = \overline{I_i} + 3\sigma_i \quad (1)$$

ACPD
11, 531–566, 2011

In which $\overline{I_i}$ is the mean baseline intensity in fluorescence channel i and σ_i is its standard deviation. The threshold therefore represents the minimum fluorescence intensity that can be reliably measured by the WIBS3. Assuming a continuous baseline distribution, this criterion is likely to misclassify ~0.5% of non-fluorescent particles as fluorescent in each channel, which should be considered when non-fluorescent particles dominate in an environment. Some sections of the analysis require dual-channel fluorescence from a particle, which reduces this probability to $\sim 10^{-6}$. The baseline is also subtracted before any comparisons of fluorescence intensity are made.

Single-particle data was binned to 15-min resolution and number concentration was calculated based on the measured aerosol sampling rate of the instrument ($0.23\,\mathrm{l\,min^{-1}} \pm 5\%$). If a second particle passes through the WIBS3 within ~10 ms of the first, the Xenon lamps will not have had time to recharge following the first, and this particle would not be classified. To ensure accurate counting the second particle is recorded as "missed" by the laser particle detection system. This was typically 10% of all particles at each site. This information is used to scale the derived fluorescent and non-fluorescent number concentrations.

A minimum elastic scattering pulse duration and intensity threshold are set to stop the WIBS3 counting brief noise spikes as aerosol particles. This threshold was raised from its default value (that used in Borneo) in Manchester because of transient rises in the noise floor (lasting ~1 min) that led to large concentrations of nonexistent "0.3–0.5 µm" aerosol triggering the Xenon lamps at their maximum rate. Outside of these events the noise floor was similar to that in Borneo. The result of permanently raising the threshold in Manchester is that the counting efficiency in the size range $0.8\,\mu\mathrm{m} \leq D_P \leq 1.6\,\mu\mathrm{m}$ is reduced when the noise events were not occurring. Comparisons with another optical particle counter (GRIMM Inc. Dust Monitor, model 1.108) show that the approximate maximum reduction is 50% at $0.8 \leq D_P \leq 1\,\mu\mathrm{m}$, 20% at $1 \leq D_P \leq 1.6\,\mu\mathrm{m}$. Larger particles appear unaffected.

Seven different particle categories are specified in the analysis, based on whether or not fluorescence is observed in each channel. These are listed in Table 1. Some

ACPD
11, 531–566, 2011

particles emit fluorescence with enough intensity to saturate the relevant WIBS3 detection channel and these particles are excluded from the analysis (except for being counted in the total number concentration, N_{tot}). The abundance of these particles is usually marginal, ranging from 0.008% to 3% of N_{tot} in the size range $0.8 \leq D_P \leq 20$ µm, and is expressed in Table 2 as a percentage of N_{tot} and of the number of fluorescent particles in that channel. The number fraction of saturating particles is most significant at $D_P > 6$ µm. Such particles generally did not exist in large enough numbers to influence the results of this analysis except in the case of F1 in the Borneo data set, where they dominated the number concentration in the size range 10–20 µm (Fig. 6viii) and account for over 20% of particles at $D_P \geq 8$ µm.

2.4 Site descriptions

Manchester is a medium-sized city (estimated population 483 000 – Manchester City Council, 2009) in the North-West of England. The WIBS3 and filter sampler were located 15 m above ground level on a measurement platform at the Centre for Atmospheric Science, University of Manchester. The building is situated approximately 1 km from the centre of Manchester, 50 m from Oxford Road (one of the main traffic routes to and from the city centre) and 8–12 km from the outer ring road that approximately denotes the urban area. A number of small parks and greens lay 1–2 km from the university, and extensive heath land is present beyond 15 km to the West of the city centre. Data was collected from the 4–21 December 2009.

Data was collected in Danum valley, N.E. Borneo, from April–May and June–July 2008 as part of the OP3/ACES intensive campaigns (a project overview is available in Hewitt et al., 2010) at a site around 60 km west of the nearest town (Lahad Datu). The WIBS3 inlet was situated 2 m above the forest floor beneath the canopy of a tropical rain forest with a typical tree height of 32 m. The three weeks of data obtained in the June–July campaign is used in this work as its nature has been discussed in detail in Gabey et al. (2010). It is thought to represent an environment rich in fungal spores in the afternoon and evening, with higher non-biological aerosol concentrations present

ACPD
11, 531–566, 2011

in the middle of the day.

3 Results and discussion

3.1 Size distribution and number concentration of fluorescent particles

3.1.1 Manchester WIBS results

The time series of N_{tot} (upper panel) and N_{F1}, N_{F2} and N_{F3} (lower panel) are plotted in Fig. 1 with shaded areas that represent periods when the filter sampler was running. Throughout December N_{non} is an order of magnitude larger than any of the fluorescent concentrations at 900–2100 l^{-1}, N_{F1} is typically 0–100 l^{-1}, N_{F2} is typically 0–200 l^{-1} and N_{F3} is typically 0–300 l^{-1}. Elevated number concentrations also occur on several days, during which N_{F1} exceeds 1000 l^{-1} with N_{F2} and N_{F3} also strongly enhanced for 1.5 days from the 10–12 December.

Data coinciding with filter collections are summarised by a box-and-whisker plot in Fig. 2i,iii with the plots for the overall dataset in Fig. 2ii,iv. Median N_{non} is smaller during filter sampling periods and the median fluorescent number concentrations are larger. Both of these changes are within their respective inter-quartile ranges but amount to a doubling in the fluorescent number fraction during filter sampling. Linear regressions of number concentration during filter sample periods show that N_{F1}, N_{F2} and N_{F3} represented 5%, 10% and 19% of N_{tot} respectively whereas for the overall dataset these figures reduce to 3%, 6% and 11% of N_{tot}. The material on the filters is therefore considered to be typical of that found in Manchester during December 2009.

A clear diurnal cycle of N_{tot} is not exhibited in Manchester, but the number concentration of all fluorescent particle types typically begins to increase at 07:00 LT , with the median values peaking at N_{F1}=75 l^{-1}, N_{F2}=100 l^{-1} and N_{F3}=200 l^{-1} at 10:00 LT after which each fall sharply by between 30% and 50%. The remainder of the cycle is characterised by lower number concentrations from 11:00 to 21:00 LT. N_{non} remains

ACPD
11, 531–566, 2011

consistent throughout the day with only small variations relative to its large day-to-day variability. It shows a slight increase at 07:00–10:00 and 17:00–19:00 LT, coinciding with locally sourced accumulation mode and coarse mode aerosol from traffic activity as rush-hours take place. This suggests that traffic activity contributes a quantity of fluorescent particles to the total number, either through resuspended PBA or PAH in aggregates. In the size interval $1.5 \leq D_P \leq 3\,\mu m$ the typical number concentrations of N_{F1}, N_{F2} and N_{F3} are 10–20 l^{-1}, 18–21 l^{-1} and 25–50 l^{-1}, respectively. In this size range the fluorescent particle mid-morning peak occurs and is accompanied by a peak in N_{non} connected with a rise that begins at 06:00 LT.

Number size distributions ($dN/d\log D_P$) of each particle type in Manchester are plotted in Fig. 3, along with the median number fraction N/N_{tot} of each particle type. Throughout the measurement period N_{non} (Fig. 3ii) dominates N_{tot} (Fig. 3ii) and both size distributions peak at 1.2 µm. The N_{non} number fraction reduces with increasing size and shows there are rarely non-fluorescent particles at $D_P \geq 9\,\mu m$.

Each fluorescent number distribution N_{F1}, N_{F2} and N_{F3} (Fig. 3iii–v) contains a primary size mode at 1.2 µm and a secondary mode at $1.5 \leq D_P \leq 3\,\mu m$ which is around half the strength. The primary fluorescent size modes in N_{F1}, N_{F2} and N_{F3} respectively account for 1.3%, 2.5% and 5% of N_{tot} and the fluorescent number fractions generally increase with particle size, peaking at 8–10 µm with values of 20%, 60% and 60%, respectively. The difference between N_{F1} and N_{F3} fractions at large sizes indicates the additional discrimination that a channel dedicated to Tryptophan-like fluorescence can provide.

The size distributions of particles exhibiting fluorescence in two channels are plotted in Fig. 3vi,vii. While qualitatively similar to the fluorescent size distributions the 1.2 µm mode reduces further and becomes comparable in strength to the 2–3 µm mode. Each peak in the $N_{F1\text{ and }F2}$ and $N_{F1\text{ and }F3}$ distributions represents an absolute particle concentration of around 10 l^{-1}. The number fraction of N_{F1} is dominated by uncertainty from the chosen fluorescence baseline (0.5% of N_{tot}) at small sizes but the presence of the same size mode in $N_{F1\text{ and }F3}$ shows that this uncertainty is not solely responsible

ACPD
11, 531–566, 2011

for the 1.2 µm mode in the N_{F1} distribution. The peak in $N_{F1\ and\ F3}$ and $N_{F1\ and\ F2}$ fractions with particle size are both 10% at 6 µm before reducing to 0 at $D_P \geq 9$ µm. The same features are present in the distributions obtained before and during filter measurements, with the higher than average fluorescent number concentration manifested as an enhancement in number across all sizes.

3.1.2 Electron microscope analysis of filter samples

Material was collected onto substrates in Manchester during the periods marked in grey in Fig. 1. To gain an impression of the dominant particle sources in Manchester, 105 particles larger than approximately 1 µm were chosen manually for imaging and EDX analysis, with an emphasis on finding different morphologies. A further 50 particles were imaged without EDX analysis and revealed two further PBA candidates. The most prominent signal peaks in the EDX spectra collected corresponded to the elements Al, C, Ca, Cl, Fe, O, S and Si.

As a basic classification scheme the relative height of these peaks was recorded and the particles sorted into basic classes based on the biggest peak. If the second largest peak height was more than 50% of the first, this was classed separately. The abundance of each class is displayed as a pie chart in Fig. 4, with Carbon, Calcium, Silicates and Iron Oxide dominating the collected spectra. The recorded images show that the carbon-rich particles are dominated by soot across the size range 1–10 µm, with the notable exception of three particles sized 3–5 µm that appear to be PBA.

Based on this information the majority of ambient aerosol in Manchester is derived from anthropogenic sources, dust transport and sea-salt (based on the presence of cube-shaped particles). A quantitative result from this analysis cannot be inferred because of uncharacterised particle losses and a manual selection process biased towards maximising the range of particle morphologies. Despite the limited dataset PBA is not thought to play a significant role at $D_P > 1$ µm in Manchester based on the EDX data and the morphology of all 155 particles.

ACPD
11, 531–566, 2011

3.1.3 Borneo WIBS results

We have further examined the data collected in a tropical rainforest in Borneo, Malaysia, described by Gabey et al. (2010). The time series of N_{tot}, N_{non} and fluorescent number concentrations found beneath the canopy are printed in Fig. 5. A strong fluorescent particle diurnal behaviour dominates N_{tot} and both N_{F1} and N_{F3} peak at 1000–2000 l^{-1} each day through a series of regular transient spikes that begin at 15:00 LT and lead to elevated concentrations through the evening. Similar spikes were recorded throughout the day when the WIBS3 inlet was placed several centimetres above a nearby patch of lichen. These features are also present in N_{F2} but its diurnal cycle peaks at 300–400 l^{-1}. Enhanced N_{non} accompanies the mid-afternoon peaks in fluorescent number, and these particles were attributed to the same source. The similarity between N_{F1} and N_{F3} is striking: 85% of Tryptophan-like particles also exhibit NADH-like fluorescence in Borneo. The concentration of fluorescent material reaches its minimum of ~50 l^{-1} during the mid-morning.

During daylight N_{non} generally remains constant or increases so that it dominates N_{tot}. Gabey et al. (2010) conclude, using various measurements both above and below the canopy, that most of the fluorescent material comprises fungal spores released between the forest floor and the canopy. This dataset is therefore considered to represent an environment where the N_{tot} is dominated by PBA.

The size distribution of each Borneo particle type is printed in Fig. 6 along with the fraction of N_{tot} it represents (dashed line). The typical N_{tot} is dominated by a strong mode at 2–3 µm with a weaker mode at 1.2 µm. The inter-quartile range shows that each size mode is subject to a high degree of variation, consistent with the changes in number concentration shown in Fig. 5.

The N_{non} size distribution (Fig. 6ii) peaks at 1.2 µm, accounting for 80% of N_{tot} at this size. The non-fluorescent material associated with PBA emission is the reason for the size mode extending to 4 µm. The N_{non} proportion increases at D_P>4 µm and reaches 15% at 9 µm. The fluorescent number fraction plateaus in the same size range,

ACPD
11, 531–566, 2011

reflecting the introduction of non-fluorescent particles.

The 2–3 µm N_{tot} mode (Fig. 6i) consists mostly of fluorescent material, with N_{F1} and N_{F3} (Fig. 6iii, v) each accounting for 80%. The relative weakness of N_{F2} (Fig. 6iv) is reflected by its size mode being smaller. It also peaks at 4 µm rather than 3 µm, probably because the measured fluorescence intensity is lower in F2 than in F1 and F3, which has implications for the fluorescent particle detection rate at smaller sizes.

The size distributions of particles exhibiting fluorescence in two channels are limited by whichever channel reports the smallest fluorescent number, however including saturating particles (Fig. 6viii) produces similar results to the N_{F3} size distribution in N_{F1} and $N_{F1\ and\ F3}$ (Fig. 6vi). The $N_{F1\ and\ F3}$ and N_{F1} distributions therefore both peak at 2–3 µm and the $N_{F1\ and\ F2}$ (Fig. 6vii) and N_{F2} distributions both peak at 4 µm. $N_{F1\ and\ F3}$ is typically greater than 75% of N_{F1} and likewise for $N_{F1\ and\ F2}$ and N_{F2}.

3.1.4 Comparison of the size spectra between sites

The number concentration and size distribution of fluorescent particles in Manchester and Borneo differ significantly: N_{F1} and N_{F3} are comparable in Borneo and primarily occupy a 2–5 µm size mode whereas in Manchester the primary mode is at 1.2 µm and N_{F1} and N_{F3} differ by a factor of 2–3 in favour of N_{F3}. In Borneo N_{F2} is around 25% of N_{F1} but N_{F2} consistently exceeds N_{F1} in Manchester, suggesting a different aerosol composition in Manchester. The Borneo number fluorescent fractions exhibit a much stronger variation with size than in Manchester. This difference exemplifies the effect of a strong local PBA source on a size distribution. One surprising feature in the Manchester dataset is that while all particles larger than 9 µm are fluorescent, few emit in multiple WIBS3 detection channels. The same cannot be said of the Borneo dataset.

Both Manchester and Borneo have a contribution of fluorescent material in all three channels at D_P>1.6 µm and the largest particle sizes are dominated by fluorescent material. This implies a significant ambiguity in ability to ascribe fluorescence solely to PBA as the majority of the Manchester coarse mode aerosol is, as indicated by the ESEM data, non-PBA and the fluorescent aerosol contains a contribution from traffic

ACPD
11, 531–566, 2011

activity.

3.2 Fluorescence intensity at each site

3.2.1 The dependence of fluorescence intensity on particle size

The dependence of measured fluorescence intensity on D_P in several channels offers information on the homogeneity of the aerosol population. For example, if fluorescence does not increase monotonically then it is unlikely that the same material is contributing at all sizes.

The dependence of fluorescence intensity on particle size in each fluorescence channel is plotted in Fig. 7i–iii for Borneo and Fig. 7iv–vi for Manchester. All six curves show a general intensity increase with particle size. This rise is confined to a narrower range of values in Borneo than in Manchester, and a number of features unique to each location are present:

F1 intensity (Fig. 7i,iv) rises steadily in the interval $0.8 \leq D_P \leq 4\,\mu m$ in both locations. Beyond this size it decreases in Manchester whereas in Borneo it continues to rise until a plateau is reached at 7 µm. This reduction in F1 intensity at $D_P \geq 6\,\mu m$ is the reason for the lack of dual-channel fluorescence from larger particles in Manchester.

F2 intensity (Fig. 7ii,v) in Borneo is distinct from F1 and F3. Rather than rising steadily with D_P it falls by 20% from 0.8 to 2 µm, rising almost linearly with D_P at larger sizes. The shaded region on the plot shows that over 10% of fluorescent 1–2 µm particles emit fluorescence as intense as that from 4–8 µm particles. It is likely the particles here are of a different type to their larger counterparts and this was not established in Gabey et al. (2010). The Borneo F2 intensity is generally 50–300 a.u. whereas in Manchester it occupies a large range throughout the size spectrum. Despite this variability the median intensity in the size interval $0.8 \leq D_P \leq 4\,\mu m$ remains almost constant with a value less than 250 a.u. in Manchester unlike the systematic increase observed in Borneo at $D_P > 2\,\mu m$. At $D_P \geq 4\,\mu m$ the F2 increase is approximately linear with with D_P.

ACPD
11, 531–566, 2011

F3 intensity (Fig. 7iii) in Manchester contains a similar enhancement to F2 at $1 \leq D_P \leq 2\,\mu m$, and is similar in its range of values, although it reduces slightly at $3 \leq D_P \leq 4\,\mu m$ and increases more strongly at larger sizes. In Borneo (Fig. 7vi) the rise in F3 is qualitatively similar to that in F1 albeit smaller in magnitude. There is no enhancement at 1–2 µm corresponding to that found in F2 (Fig. 7v) despite the common detection wavelengths. Hill et al. (2009) note that excitations at sub-315 nm are required to induce fluorescence in water-borne bacterial cells, and at around 1 µm the particle is consistent with some bacteria classes. This is a possible explanation for the feature in the Borneo understorey, which features an abundant source of biological material and a consistently damp environment.

3.2.2 The F1:F3 intensity ratio in Borneo and Manchester

In particles emitting fluorescence in F1 and F3 the ratio F1/F3 of fluorescence intensity describes the relative amount of Tryptophan-like to NADH-like material in each particle. Figure 8i,ii shows the F1 and F3 intensity in Borneo when non-saturating fluorescence was recorded in both channels while Fig. 8iii shows the fluorescence intensity ratio F1/F3. As in the general case both F1 and F3 both rise with particle size and plateau at 6 µm. The F3 curve plateaus more clearly than in the general case because saturating F1-type particles are excluded, which removes some higher-intensity F3-type particles.

The ratio F1/F3 is log-normally distributed and its median does not vary significantly from log(F1/F3)=0.5 in the size range $1.5 \leq D_P \leq 10\,\mu m$. At D_P=0.9 µm log(F1/F3) decreases to 0.4 and the difference between the 10th and 90th percentile is 1.8 orders of magnitude. The range of F1/F3 values shrink to 1.2 orders of magnitude at $D_P \geq 3\,\mu m$. The reason for this is the standard deviation of the WIBS3 fluorescence baseline, which is 20–30 a.u. in all channels. This is comparable to the intensity recorded at small sizes and so is affected by random fluctuations.

Figure 8iv-vi shows the equivalent plots for Manchester. The F1 intensity vs. D_P plot in Fig. 8 is similar to the general case in Manchester (Fig. 7i), but the F3 intensity now ranges from 300–750 a.u. at $2\,\mu m \leq D_P \leq 10\,\mu m$ and there is a clear rise with D_P

ACPD
11, 531–566, 2011

throughout the size range, unlike in the general case. A minimum F3 intensity appears to be required before any fluorescence is observed in F1, suggesting the F1 channel is effectively less sensitive than the F3 channel.

In Manchester, log(F1/F3) is 0.5–1 order of magnitude smaller than in Borneo at all sizes, and rather than being constant over most values of D_P its median value rises from −0.15 to 0 at $0.9 \leq D_P \leq 2$ µm and falls to −0.5 between 2.5 and 8 µm, with the falloff in F1 intensity responsible for the latter feature. It should also be noted that the small number of fluorescent particles at larger sizes compared with Borneo increases the uncertainty in the measurement.

The structural similarities of F2 and F3 intensity vs. D_P in both locations suggest that the majority of fluorescence recorded in the F2 channel results from the same fluorescent molecules (or the same process that allows particles to accumulate fluorophores) as in the F3 channel. It is also noteworthy that $N_{F3} > N_{F2} > N_{F1}$ in Manchester. The divergence of F1 and F3 intensity at $D_P > 4$ µm is interesting because it is generally assumed that the fluorescence intensity of particles increases significantly with particle size since a 10 µm particle contains 1000 times the volume of a 1 µm particle. Since the curves are dictated by whatever fluorescent particle type dominates the number concentration, it is likely that at least two such particle types are present in Manchester.

The reason for the specific value of the ratio F1/F3 is not known but it relates to the fluorescence quantum yield of different fluorophores, the presence of interferents or the way in which the fluorescent material is arranged inside the aerosol particle, as well as instrument calibration. Nevertheless the general size independence of F1/F3 in Borneo is noteworthy and suggests the same type of particles (fungal spores) dominate the fluorescent size spectrum, unlike in Manchester.

3.2.3 The F1:F2 intensity ratio in Borneo and Manchester

Similar results to the F1/F3 ratio were obtained in both locations when the ratio F1/F2 was calculated as a function of size. In particles emitting fluorescence in both F1 and

ACPD
11, 531–566, 2011

F2 the curves of fluorescence intensity and F1/F2 vs. DP at each site (Fig. 9i–vi) are similar in form to those in Fig. 8, albeit with two structural differences: Firstly, a plateau in Manchester F2 intensity at 2–3 µm (Fig. 9v) causes the F1/F2 curve (Fig. 9vi) to peak at 3 µm rather than 2 µm. Secondly, in the Borneo dataset F2 intensity (Fig. 9ii) is higher at 0.9 µm than at 1.2m, after which it increases with DP whereas F3 intensity (Fig. 8ii) increases monotonically throughout. This produces a steeper F1/F2 curve at $0.9 \leq D_P \leq 1.2$ µm compared with F1/F3.

In Borneo "F1 and F2" particles, F2 intensity (Fig. 9ii) is suppressed relative to the general case for F2 (Fig. 7ii), reaching maxima of 60 and 200 a.u. respectively at D_P >5 µm. F3 intensity from "F1 and F3" particles (Fig. 8ii) is also less than in the general case (Fig. 7iii) in Borneo. The reduction is likely to be caused by the exclusion of saturating F1-type particles, which removes higher-intensity F3-type particles. The number of saturating particles in Manchester is smaller than in Borneo, and F2 intensity from "F1 and F2" type particles (Fig. 9v) is modally higher than in the general "F2" case (Fig. 7v), reaching a maximum of 500 a.u. rather than 250 a.u. The same is true of Manchester F3 intensity from "F1 and F3" type particles (Fig. 8v), which reach 1000 a.u. compared with 500 a.u. in the general case (Fig. 7v).

4 Further discussion

A potential use for the fluorescence ratio recorded in a high-PBA environment is to use it as a set of upper and lower threshold values to identify similar material in a low-PBA environment. To demonstrate this, the Manchester fluorescence data was limited to those particles with an intensity ratio F1/F3 within the inter-quartile range of that found in Borneo (Fig. 8iii) for each D_P bin. The typical resulting concentration of "Borneo-like" particles in Manchester was limited to 2–19 l^{-1} (10th and 90th percentiles), with size modes at 1.2 µm and 2–3 µm. A non-zero concentration is unsurprising despite the differing environments because of the broad range of F1/F3 ratios found in Manchester.

ACPD
11, 531–566, 2011

It is clear that, at $D_P \geq 2$ µm, the F2 and F3 channels detect the same fluorophores (albeit with differing degrees of success) since both exhibit a similar relationship with D_P in both locations whereas the corresponding plots of F1 intensity are distinct. Both datasets also contain features reflecting the finding that fluorescence intensity is not necessarily proportional to particle size in ambient urban aerosol.

The measurements using channel F3 in Manchester are comparable to UV-APS measurements performed by Huffman et al. (2010) to characterise the fluorescent aerosol in Mainz, Germany, in Autumn 2006. While the measurements were carried out in different seasons and the region around Mainz contains more woodland than Manchester, the results are similar: Huffman et al. note that 25% of the aerosol larger than 4 µm (aerodynamic diameter) is likely to be fluorescent biological aerosol. The Manchester N_{F3}/N_{tot} plot (Fig. 3v) shows a similar relationship between fluorescent percentage and particle size, but we conclude that the PBA influence is marginal in Manchester. Huffman et al. note the presence of a fluorescent size mode at $D_A < 2$ µm and attribute this to PAHs confined to this size range, however the EDX and ESEM images obtained in Manchester show that soot is readily found with characteristic size up to 10 µm and the same assumption cannot be made for Manchester.

5 Summary

WIBS3 data was collected in the winter in Manchester and below the canopy of tropical rainforest in Borneo, Malaysia. The two datasets are taken to reflect a marginal PBA influence and heavy PBA influence, respectively. SEM images of super-1 µm aerosol confirm that the winter PBA contribution is small in Manchester however the small number of imaged particles means this is subject to a large uncertainty. Manchester featured a primary fluorescent mode at 1 µm and a small enhancement at 1.5–3 µm, with fluorescent aerosol equal to 11% or less of the total number in the size range 0.8–20 µm. In Borneo fluorescent aerosol sized 3–5 µm represented up to 66% of N_{tot}. The size-resolved ratios of fluorescence intensity in two pairs of fluorescence channels was

ACPD
11, 531–566, 2011

compared at the two sites and differed significantly, with the Borneo ratio only slightly dependent upon particle size whereas the Manchester ratio was heavily dependent upon it and more variable.

6 Conclusions

Fluorescent aerosol differs significantly at the two locations. In Manchester fluorescent particles number 0–300 l^{-1} whereas in Borneo they are much more abundant, at 100–2000 l^{-1}. The different sources of fluorescent material at each site are reflected by the number size distributions, which contain primary modes at 1.2 µm in Manchester and at 3–4 µm in Borneo. Tryptophan-like (F1) fluorescent particles were comparable in number to NAD(P)H-like (F3) in Borneo but were typically outnumbered 3-to-1 in Manchester. Part of this difference could be explained by the difficulty in detecting fluorescence at smaller D_P however N_{F1} remains relatively small, even at $D_P \geq 4$ µm.

The dependence between fluorescence intensity and D_P in the three WIBS3 fluorescence channels cannot be described with a simple relationship because each has strong features at certain sizes. However, the apparently linear relationship between intensity and D_P across ranges of several microns in each case is surprising given that the fluorescence from homoegeneous clusters of bacteria generally increases with D_P^2 (Hill et al., 2001).

In Manchester the divergence in F1 and F3 intensity at $D_P > 4$ µm demonstrates that the F1 channel offers better discrimination than the F3 channel in an aerosol population influenced by likely fluorescent non-PBA. Despite the high biodiversity of the tropical rainforest, the range of fluorescence intensities found in Borneo is more limited than in Manchester, where it exhibits greater variation across all particle sizes. This reflects the probable diversity of sources in Manchester compared with locally produced fungal spores.

Particles exhibiting fluorescence in channels F1 and F3 in the urban and PBA-dominated environments can be discriminated based on the characteristics of the

ACPD
11, 531–566, 2011

F1/F3 vs. D_P curves in each location. This ratio initially rises with particle size before becoming largely invariant at $D_P \geq 1.5\,\mu m$ in Borneo. In Manchester the median log(F1/F3) peaks at 0 ($D_P = 2\,\mu m$) and the inter-quartile range is ~1 compared with a median value of 0.5 across most sizes and an inter-quartile range of ~0.5 in Borneo. The results obtained from Borneo can be used to select "Borneo-like" particles in Manchester, where $\sim 10\,l^{-1}$ are found to be similar.

Acknowledgement. This work was funded by the Natural Environment Research funded projects "Aerosol Characterisation Experiment" (ACES) (contract # NE/E011233/1), part of the NERC APPRAISE programme (Aerosol Properties, Processes And Influences on the Earth's Climate), and the NERC Oxidant & Particle Photochemical Processes Tropical Rain Forest (OP3) project contract # NE/D004624/1. We thank the Malaysian and Sabah Governments for their support; the Malaysian Meteorological Department (MMD) for access to the Bukit Atur Global Atmosphere Watch station; W. Sinun of Yayasan Sabah and his staff; and G. Reynolds of the Royal Society's South East Asian Rain Forest Research Programme and his staff for logistical support at the Danum Valley Field Centre. Mr. Gabey is in receipt of a NERC studentship. Thanks are also due to R. Burgess, Centre for Atmospheric Science, Manchester, for her assistance with the ESEM analysis.

References

Agranovski, V., Ristovski, Z., Hargreaves, M., Blackall, P. J., and Morawska, L.: Real-time measurement of bacterial aerosols with the UVAPS: performance evaluation, J. Aerosol Sci., 34, 301–317, 2003a.

Agranovski, V., Ristovski, Z., Hargreaves, M., Blackall, P. J., and Morawska, L.: Performance evaluation of the UVAPS: influence of physiological age of airborne bacteria and bacterial stress, J. Aerosol Sci., 34, 1711–1727, 2003b.

Diehl, K., Quick, C., Matthias-Maser, S., Mitra, S. K., and Jaenicke, R.: The ice nucleating ability of pollen: Part I. Laboratory studies in deposition and condensation freezing modes, Atmos. Res., 58, 75–87, 2001.

Diehl, K., Matthias-Maser, S., Jaenicke, R., and Mitra, S. K.: The ice nucleating ability of pollen:

ACPD

11, 531–566, 2011

Part II. Laboratory studies in immersion and contact freezing modes, Atmos. Res., 61, 125–133, 2002.
Faris, G. W., Copeland, R. A., Mortelmans, K., and Bronk, B. V.: Spectrally resolved absolute fluorescence cross sections for bacillus spores, Appl. Opt., 36, 958–967, 1997.
Foot, V. E., Kaye, P. H., Stanley, W. R., Barrington, S. J., Gallagher, M., and Gabey, A.: Low-cost real-time multiparameter bio-aerosol sensors, Optically Based Biological and Chemical Detection for Defence IV, Cardiff, Wales, UK, 71160I-71112, 2008.
Gabey, A. M., Gallagher, M. W., Whitehead, J., Dorsey, J. R., Kaye, P. H., and Stanley, W. R.: Measurements and comparison of primary biological aerosol above and below a tropical forest canopy using a dual channel fluorescence spectrometer, Atmos. Chem. Phys., 10, 4453–4466, doi:10.5194/acp-10-4453-2010, 2010.
Gilbert, G. S. and Reynolds, D. R.: Nocturnal fungi: airborne spores in the canopy and understory of a tropical rain forest, Biotropica, 37, 462–464, 2005.
Hewitt, C. N., Lee, J. D., MacKenzie, A. R., Barkley, M. P., Carslaw, N., Carver, G. D., Chappell, N. A., Coe, H., Collier, C., Commane, R., Davies, F., Davison, B., DiCarlo, P., Di Marco, C. F., Dorsey, J. R., Edwards, P. M., Evans, M. J., Fowler, D., Furneaux, K. L., Gallagher, M., Guenther, A., Heard, D. E., Helfter, C., Hopkins, J., Ingham, T., Irwin, M., Jones, C., Karunaharan, A., Langford, B., Lewis, A. C., Lim, S. F., MacDonald, S. M., Mahajan, A. S., Malpass, S., McFiggans, G., Mills, G., Misztal, P., Moller, S., Monks, P. S., Nemitz, E., Nicolas-Perea, V., Oetjen, H., Oram, D. E., Palmer, P. I., Phillips, G. J., Pike, R., Plane, J. M. C., Pugh, T., Pyle, J. A., Reeves, C. E., Robinson, N. H., Stewart, D., Stone, D., Whalley, L. K., and Yin, X.: Overview: oxidant and particle photochemical processes above a south-east Asian tropical rainforest (the OP3 project): introduction, rationale, location characteristics and tools, Atmos. Chem. Phys., 10, 169–199, doi:10.5194/acp-10-169-2010, 2010.
Hill, S. C., Pinnick, R. G., Niles, S., Fell, N. F., Pan, Y.-L., Bottiger, J., Bronk, B. V., Holler, S., and Chang, R. K.: Fluorescence from airborne microparticles: dependence on size, concentration of fluorophores, and illumination intensity, Appl. Opt., 40, 3005–3013, 2001.
Hill, S. C., Mayo, M. W., and Chang, R. K.: Fluorescence of Bacteria, Pollens, and Naturally Occurring Airborne Particles: Excitation/Emission Spectra, Army Research Laboratory, 2009.
Ho, J.: Real time detection of biological aerosols with fluorescence aerodynamic particle sizer (FLAPS), J. Aerosol Sci., 27, 581–582, 1996.
Huffman, J. A., Treutlein, B., and Pöschl, U.: Fluorescent biological aerosol particle concentrations and size distributions measured with an Ultraviolet Aerodynamic Particle Sizer (UV-

ACPD
11, 531–566, 2011

APS) in Central Europe, Atmos. Chem. Phys., 10, 3215–3233, doi:10.5194/acp-10-3215-2010, 2010.
Kaye, P., Stanley, W. R., Hirst, E., Foot, E. V., Baxter, K. L., and Barrington, S. J.: Single particle multichannel bio-aerosol fluorescence sensor, Opt. Express, 13, 3583–3593, 2005.
Lakowicz, J. R.: Principles of Fluorescence Spectroscopy, 3rd edn., Springer, New York, p. 5, 2006.
Matthias-Maser, S. and Jaenicke, R.: The size distribution of primary biological aerosol particles with radii >0.2 µm in an urban/rural influenced region, Atmos. Res., 39, 279–286, 1995.
Pan, Y.-L., Pinnick, R. G., Hill, S. C., Rosen, J. M., and Chang, R. K.: Single-particle laser-induced-fluorescence spectra of biological and other organic-carbon aerosols in the atmosphere: measurements at New Haven, Connecticut, and Las Cruces, New Mexico, J. Geophys. Res., 112, D24S19, doi:10.1029/2007JD008741 2007.
Pan, Y.-L., Hill, S. C., Pinnick, R. G., Huang, H., Bottiger, J. R., and Chang, R. K.: Fluorescence spectra of atmospheric aerosol particles measured using one or two excitation wavelengths: comparison of classification schemes employing different emission and scattering results, Opt. Express, 18, 12436–12457, 2010.
Pinnick, R. G., Hill, S. C., Niles, S., Pan, Y.-L., Holler, S., Chang, R. K., Bottiger, J., Chen, B. T., Orr, C.-S., and Feather, G.: Real-time measurement of fluorescence spectra from single airborne biological particles, Field Anal. Chem. Technol., 3, 221–239, 1999.
Pinnick, R. G., Hill, S. C., Pan, Y.-L., and Chang, R. K.: Fluorescence spectra of atmospheric aerosol at Adelphi, Maryland, USA: measurement and classification of single particles containing organic carbon, Atmos. Environ., 38, 1657–1672, 2004.
Schauer, C., Niessner, R., and Pöschl, U.: Analysis of nitrated polycyclic aromatic hydrocarbons by liquid chromatography with fluorescence and mass spectrometry detection: air particulate matter, soot, and reaction product studies, Anal. Bioanal. Chem., 378, 725–736, 2004.
Sivaprakasam, V., Huston, A., Lin, H. B., Eversole, J., Falkenstein, P., and Schultz, A.: Field test results and ambient aerosol measurements using dual wavelength fluorescence excitation and elastic scatter for bioaerosols, Chemical and Biological Sensing VIII, Orlando, FL, USA, 2007, 65540R-65547.
Uk Lee, B., Jung, J. H., Yun, S. H., Hwang, G. B., and Bae, G. N.: Application of UVAPS to real-time detection of inactivation of fungal bioaerosols due to thermal energy, J. Aerosol Sci., 41, 694–701, 2010.
Westphal, A. J., Price, P. B., Leighton, T. J., and Wheeler, K. E.: Kinetics of size changes of

ACPD
11, 531–566, 2011

individual Bacillus thuringiensis spores in response to changes in relative humidity, P. Natl. Acad. Sci. USA, 100, 3461–3466, 10.1073/pnas.232710999, 2003.
Yarwood, C. E.: Water content of Fungus spores, Am. J. Bot., 37, 636–639, 1950.

ACPD
11, 531–566, 2011

Table 1. The particle types specified in the analysis.

Short name	Description
Tot	Total number concentration
Non	No fluorescence detected in any channel
F1	Fluorescence detected in channel F1 (excitation at 280 nm, detection 310–400 nm)
F2	Fluorescence detected in channel F2 (excitation at 280 nm, detection 400–600 nm)
F3	Fluorescence detected in channel F3 (excitation at 370 nm, detection 400–600 nm)
F1andF3	Fluorescence in F1 and F3 (the "FBAP" criterion in Gabey et al., 2010)
F1andF2	Fluorescence in F1 and F2

ACPD
11, 531–566, 2011

Table 2. The contribution of particles that saturate the fluorescence detector.

	Contribution to N_{tot} (%)			Contribution to N_{FL} (same channel)		
Location	F1	F2	F3	F1	F2	F3
Borneo	3%	0.008%	0.34%	5%	0.05%	0.6%
Manchester	0.13%	0.28%	0.6%	3.2%	5.1%	5.8%

ACPD
11, 531–566, 2011

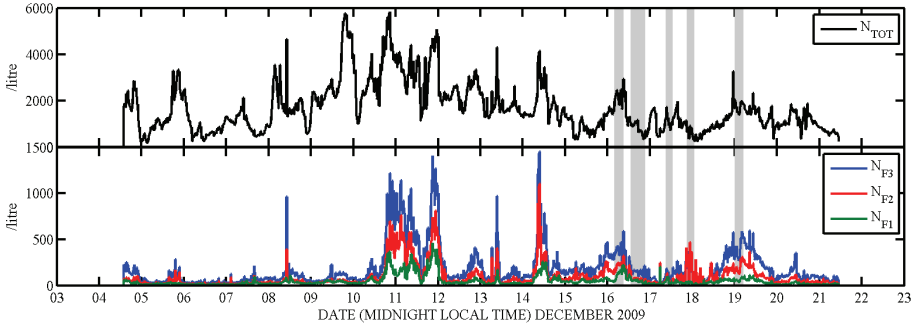

Fig. 1. Time series of WIBS3 number concentrations in Manchester 2009. Filter samples were collected in the periods marked by shaded areas.

ACPD
11, 531–566, 2011

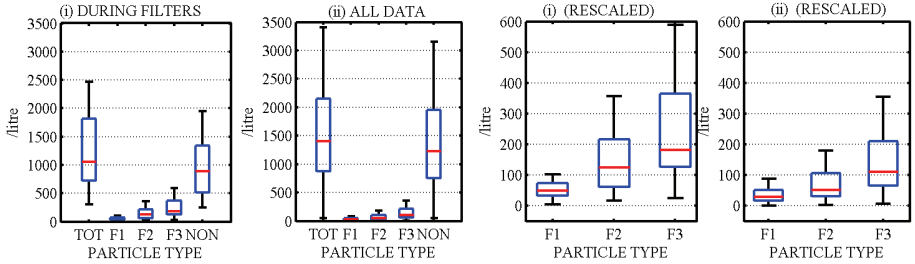

Fig. 2. Box-and-whisker plots of N_{non}, N_{tot} and fluorescent number concentrations in Manchester during filter sampling periods **(i, iii)** and overall **(ii, iv)**.

ACPD
11, 531–566, 2011

The fluorescence properties of aerosol larger than 0.8 µm

A. M. Gabey et al.

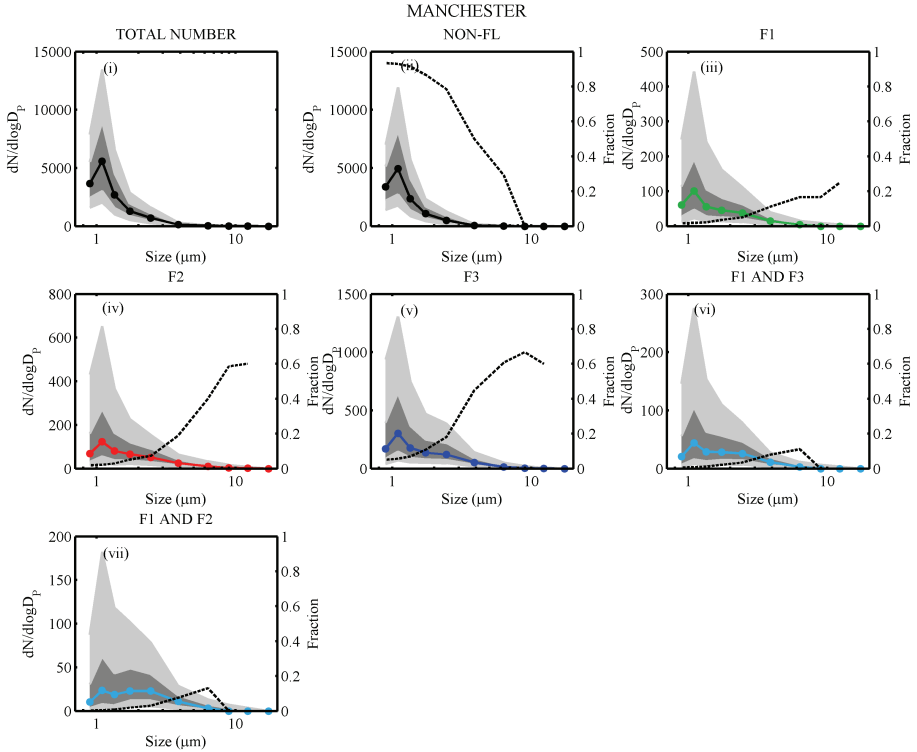

Fig. 3. Manchester number size distributions (logarithmic mid-size bins) for each particle type in Table 1. Lines denote median, dark shading: 25% and 75%, light shading: 10% and 90%. Dashed lines show median number fraction N/N_{tot}.

ACPD
11, 531–566, 2011

The fluorescence properties of aerosol larger than 0.8 μm

A. M. Gabey et al.

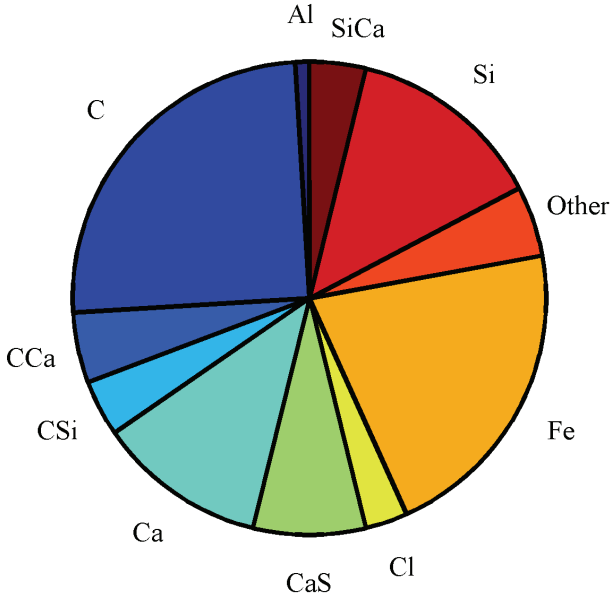

Fig. 4. The proportion of EDX spectra dominated by one or two elements.

ACPD
11, 531–566, 2011

The fluorescence properties of aerosol larger than 0.8 µm

A. M. Gabey et al.

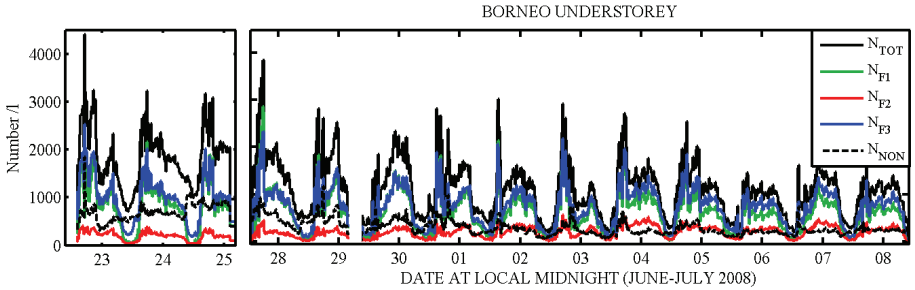

Fig. 5. Time series of WIBS3 Borneo number concentration for June–July 2008. Adapted from Gabey et al. (2010).

ACPD
11, 531–566, 2011

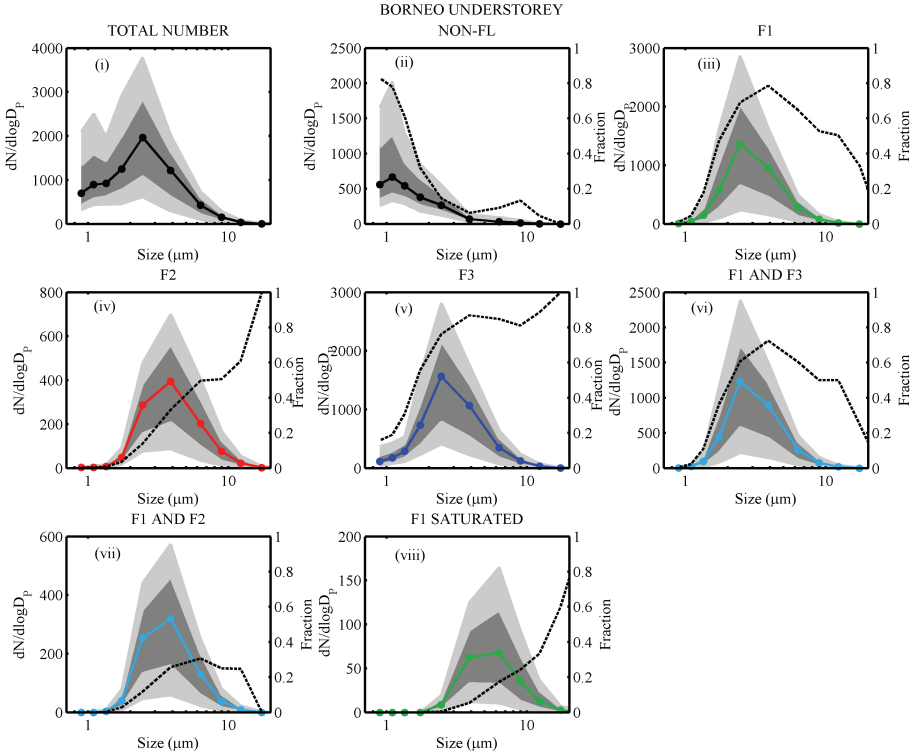

Fig. 6. Borneo number size distributions (logarithmic mid-size bins) for each particle type (Table 1). Lines represent median, dark shading: 25% and 75%, light shading: 10% and 90%. Dashed lines show median number fraction N/N_{tot}.

ACPD
11, 531–566, 2011

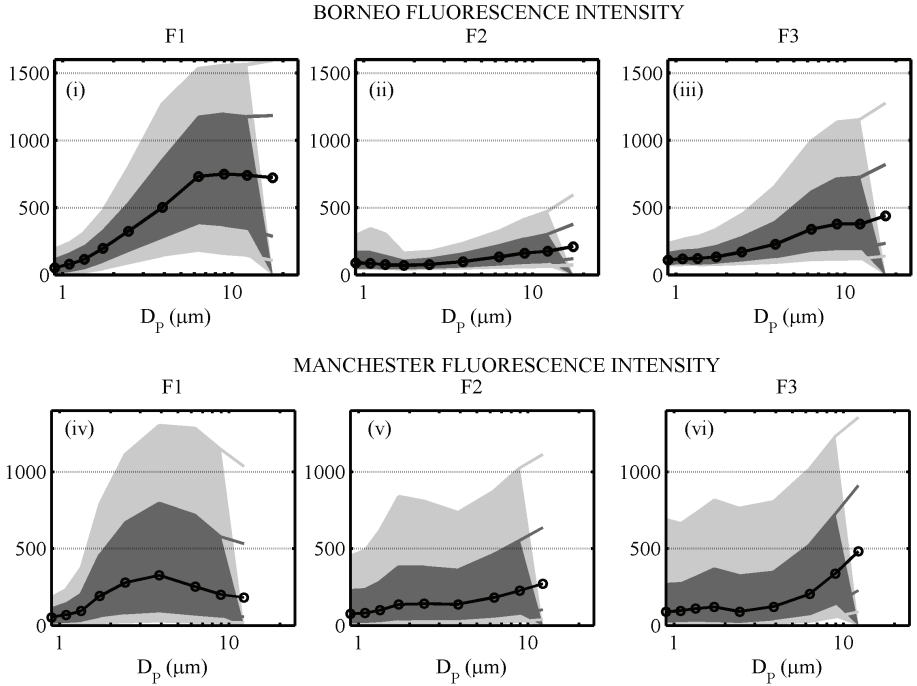

Fig. 7. Fluorescence intensity (arbitrary scale) vs. D_P (arbitrary scale) in each WIBS3 fluorescence channel in Borneo (upper panel) and Manchester (lower panel). Solid lines: median intensity, dark shading: 25% and 75%, light shading: 10% and 90%. Grey lines denote interpolated values.

ACPD
11, 531–566, 2011

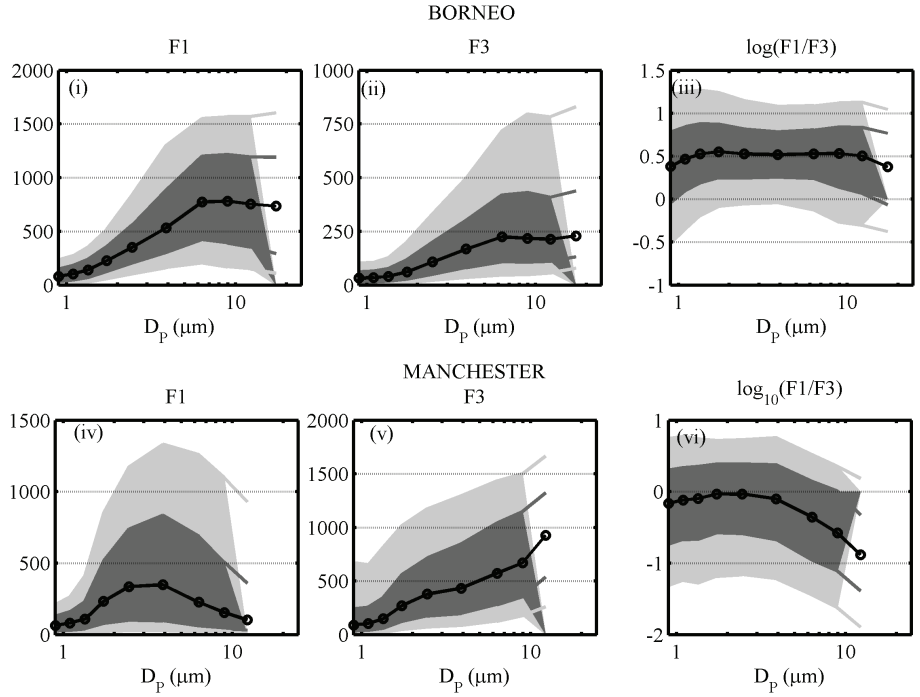

Fig. 8. Size-resolved fluorescence intensity and ratio F1:F3 in Borneo (upper panel) and Manchester (lower panel). Solid lines: median value, dark shading: inter-quartile range, light shading: 10th and 90th percentiles. Grey lines denote interpolated values.

ACPD
11, 531–566, 2011

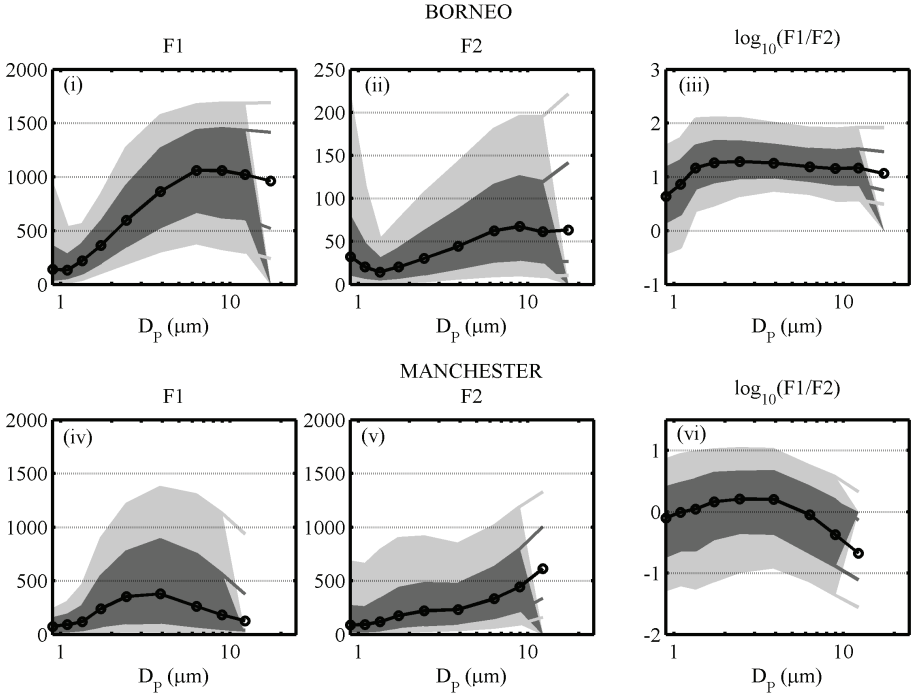

Fig. 9. Size-resolved fluorescence intensity and ratio F1:F2 in Borneo (upper panel) and Manchester (lower panel). Solid lines: median value, dark shading: inter-quartile range, light shading: 10th and 90th percentiles. Grey lines denote interpolated values.

ACPD
11, 531–566, 2011